

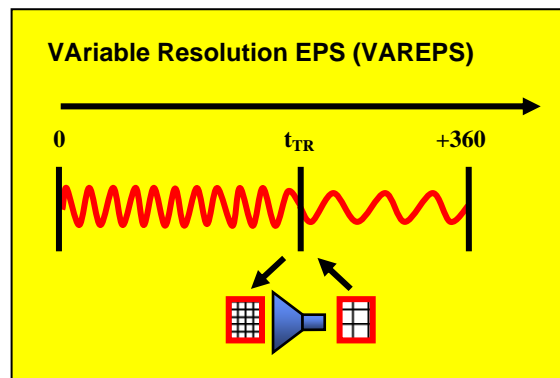
The ECMWF Variable Resolution Ensemble Prediction System (VAREPS)

*Roberto Buizza, Jean-Raymond Bidlot, Nils Wedi, Manuel Fuentes, Mats Hamrud,
Graham Holt, Tim Palmer and Frederic Vitart*

European Centre for Medium-Range Weather Forecasts, Reading UK (www.ecmwf.int)

To be published in the ECMWF NewsLetter, summer 2006

DRAFT Version v4, 27 June 2006.



1 The ECMWF Ensemble Prediction System

The Ensemble Prediction System (EPS) has been part of the ECMWF operational suite since December 1992. At that time, the EPS was based on 33 forecasts produced with a T63L19 (spectral triangular truncation T63 with 19 vertical levels) resolution version of the ECMWF model (*Molteni et al.* 1996), with initial uncertainties simulated by starting 32 members from perturbed initial conditions defined by T21L31 perturbations rapidly-growing during the first 36 hours of the forecast range (the singular vectors, see *Buizza & Palmer* 1995).

Since December 1992, the EPS have been upgraded several times: during these years, the EPS has used the same model version as the data assimilation and forecast system. Thus, it has benefited from any positive upgrade of these two. Furthermore, some model cycles included substantial changes of the EPS configuration, designed to improve both the simulation of initial and model uncertainties, the most important of which are the following:

- In 1994 the singular vectors' optimisation time interval was extended to 48 hours.
- In 1995 the singular vectors' resolution was increased to T42L31
- In 1996 the system was upgraded to a 51-member T_L159L31 system (spectral triangular truncation T159 with linear grid; *Buizza et al.* 1998), with T42L31 singular vectors.
- In 1998, initial uncertainties due to perturbations that had grown during the 48 hours previous to the starting time (evolved singular vectors, *Barkmeijer et al* 1999) were included, and a scheme to simulate model uncertainties due to random model error in the parameterised physical processes was introduced (*Buizza et al.* 1999). EPS wave forecasts became available following the introduction of the coupled atmosphere-wave model in the forecast model. (*Saetra & Bidlot* 2002, *Janssen et al* 2005).
- In 2000, following the resolution increase of the ECMWF data-assimilation and high-resolution systems from T_L319L31 to T_L511L60, the EPS resolution was upgraded to T_L255L40 (*Buizza et al* 2003), with T42L40 singular vectors. The wave model resolution was increased to a grid spacing of the order of 110 km.
- In 2002, tropical perturbations were added to the system (*Barkmeijer et al* 2001).
- In 2004, the Gaussian sampling method for generating the EPS initial perturbations using singular vectors was implemented (*Ehrendorfer & Beck* 2003).
- On 1 February 2006, following another resolution increase of the ECMWF data-assimilation and high-resolution systems to T_L799L90, the EPS resolution was further increased to T_L399L62 (see the article by *Untch et al* published in this News Letter), with T42L62 singular vectors. The wave model spectral resolution was increased to 30 frequencies and 24 directions respectively without any change to its horizontal resolution.

The most recent change is the first of a 3-phase upgrading process that will lead to the implementation of the ECMWF Variable Resolution Ensemble Prediction System (VAREPS), designed to increase the ensemble resolution in the early forecast range and to extend the forecast

range covered by the ensemble system initially to 15 days and eventually to one month, following the planned merging the ensemble and the monthly operational system:

- Phase 1 (Feb 2006): resolution increase of the 10-day EPS from T_L255L40 to T_L399L62
- Phase 2 (planned for the 2nd half of 2006): extension of the forecast range to 15 days using the VAREPS system, with T_L399L62(d0-10) and T_L255L62(d10-15)
- Phase 3 (planned for 2007): weekly extension of VAREPS to one month, with a T_L255L62 atmospheric resolution and ocean coupling introduced at day 10 (the precise configuration of this final stage of VAREPS is still to be finalized)

Only the first two phases are discussed in the present communication: the phase-3 extension to one month will be discussed in a forthcoming article.

2 The rationale behind a variable resolution approach

VAREPS aims to provide better predictions of small-scale, severe-weather events in the early forecast range, and skilful large-scale guidance in the medium forecast range. The strategy used to achieve these goals is (i) to resolve small-scales up to the forecast time when they are predictable and their inclusion has a positive impact on the forecast accuracy, and (ii) not to resolve them later in the forecast range when including them has a smaller, less detectable impact. This strategy leads to a more cost-efficient use of the computer resources, with most of them used in the early forecast range to resolve the small but still predictable scales. It is worth reminding that a similar approach to ensemble prediction is not new, since it has been used at the National Centers for Environmental Prediction (NCEP, Washington) since inception of their ensemble prediction system (add reference).

2.1 The planned operational configuration

Technically, each VAREPS perturbed member (i.e. the members starting from perturbed initial conditions and run with a stochastic simulation of random model errors) will be generated by a *2-leg forecast*, with *leg-1* run with a T_L399L62 resolution up to forecast day 10 and *leg-2* run with a T_L255L62 resolution from forecast day 9 to 15 (see Fig. 1):

- **leg-1:** T_L399L62, from day 0 to day 10
- **leg-2:** T_L255L62, from day 9 to day 15

The horizontal resolution of the wave model stays unchanged (~110 km), however leg-1 is now run with the same spectral resolution as the deterministic forecast (30 frequencies and 24 directions). The second leg reverts to 25 frequencies and 12 directions.

VAREPS will also include two other constant-resolution forecasts for calibration/validation purposes: a 15-day T_L399L62 forecast and a 15-day T_L255L62 forecast (these two extra forecasts will be added to the VAREPS suite following users' requests; they will be accessible from MARS in stream=ENFO as type=CV, number=1,2).

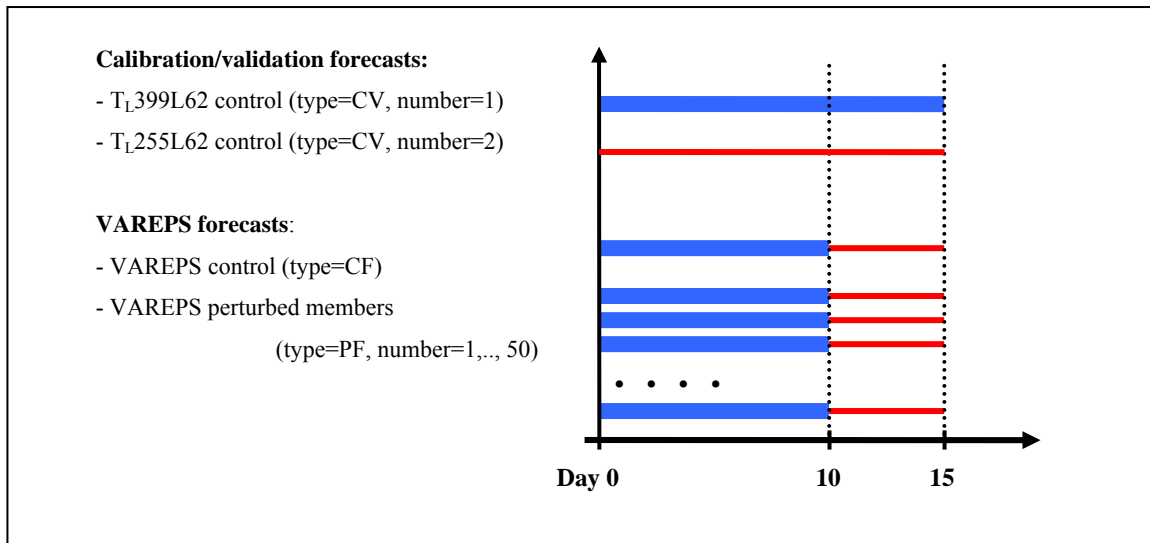


Figure 1. Schematic of VAREPS and calibration/validation forecasts that will be available after the operational implementation of VAREPS, planned for the second half of 2006.

Users should be aware of three key VAREPS technical characteristics:

- **Leg-2 initial conditions** - Each leg-2 forecast starts from a leg-1 day-9 forecast (see Fig. 2), interpolated at the T₁₂₅₅L62 resolution: this 24-hour overlap period has been introduced to reduce the impact on the fields that are more sensitive to the truncation from the high to the low resolution (e.g. convective and large scale precipitation). High resolution wave spectra are smoothed out to the lower spectral resolution of the second leg.
- **Accumulated fields** - Accumulated fields are accumulated from the start of the leg-1 forecast. To do so also in leg-2, once the leg-2 forecast reaches 24-hour, i.e. day-10 if counted from the beginning of the forecast, all leg-2 accumulated fields are overwritten by the leg-1 day-10 forecast fields, interpolated on the T₁₂₅₅ reduced Gaussian grid.
- **FDB and MARS streams ENFO and EFOV** - In the Field Data Base (FDB) and the Meteorological Archival and Retrieval System (MARS), leg-1 forecasts from day 0 to day 10, and leg-2 forecasts from day 10 to day 15 are written in the MARS stream ENFO (the Ensemble Forecast stream), while leg-2 forecasts from day 9 to day 10 are written in the new MARS stream EFOV (Ensemble Forecast Overlap stream). Similarly, ensemble wave fields are written in, respectively, streams WAEF and WEOV.

These characteristics imply that only users interested in using VAREPS forecast for accumulated fields after forecast day 10 will have to take care when constructing fields accumulated between two forecast steps that include the truncation step (see Appendix A for more details).

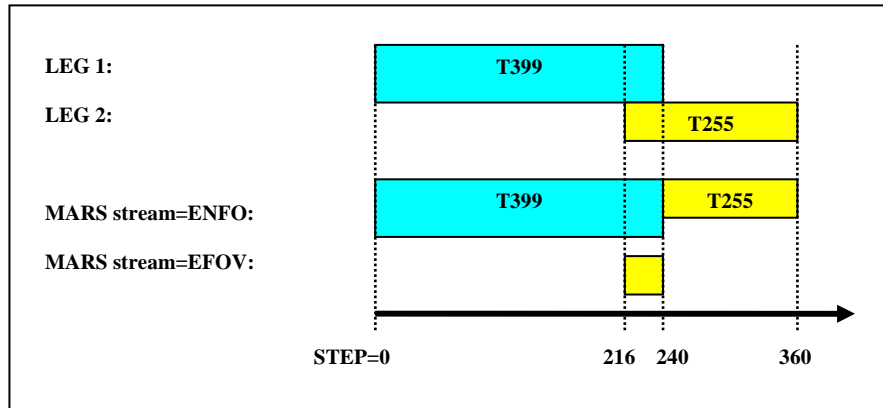


Figure 2. Schematic of the 2-leg VAREPS planned for operational implementation, with MARS data streams ENFO and EFOV.

3 Expected average impact of the introduction of VAREPS

Ensembles run with a VAREPS configuration with a day-7 truncation (a day-7 instead of the day-10 truncation was the one initially planned for operational implementation) and 40 vertical levels have been compared with two constant resolution ensemble configurations:

- T255: T_L255L40(d0-13), with a 2700 second time step (this was the EPS configuration operational before 1 February 2006)
- VAREPS: T_L399L40(d0-7) with a 1800 second time step and T_L255L40(d6-13) with a 2700 second time step
- T319: T_L319L40(d0-13) with a 1800 second time step

The second and the third configurations require ~3.5 times the computing requirements of the first configuration. Hereafter, the average performance of these configurations in providing probabilistic predictions of 500 hPa geopotential height, 850 hPa temperature and total precipitation anomalies over the Northern Hemisphere are compared. Apart for the resolution, these ensembles used the same model cycle, started from the same analysis, used the same set of initial perturbations and were based on 50 perturbed plus 1 unperturbed forecast.

3.1 T_L255(d0-13) EPS versus VAREPS T_L399(d0-7)+T_L255(d7-13)

Figure 3 shows the 60-case average area under the relative operating characteristic curve and the Brier skill score (*Wilks* 1995) for the probabilistic prediction of total precipitation in excess of 10 and 20 mm over 12 hours, for the T255 and the VAREPS systems, verified against a proxy of observed precipitation defined by the 24-hour forecast of the operational, high resolution system. These 60 cases span a 5-year period, and include both severe and non severe event cases (in selecting these cases care was taken not to introduce any bias in the sample). Each panel of this figure also shows the value of the rank-sum Mann-Whitney-Wilcoxon (RMW) significance test (computed using a

bootstrapping technique): this test measures the probability that the distributions of scores for the systems may come from the same overall population. For example, RMW values of 10% (right axis) indicate that there is a 10% chance that the two scores' distributions coincide. Figure 3 shows that VAREPS has higher average scores than T255 up to forecast day 7 for the 10 mm/12h threshold, and day 5 for the 20 mm/12h threshold, with RMW values below 10% in the first and 20% in the second case. Results also indicate that after the truncation step the difference between the two systems is not statistically significant.

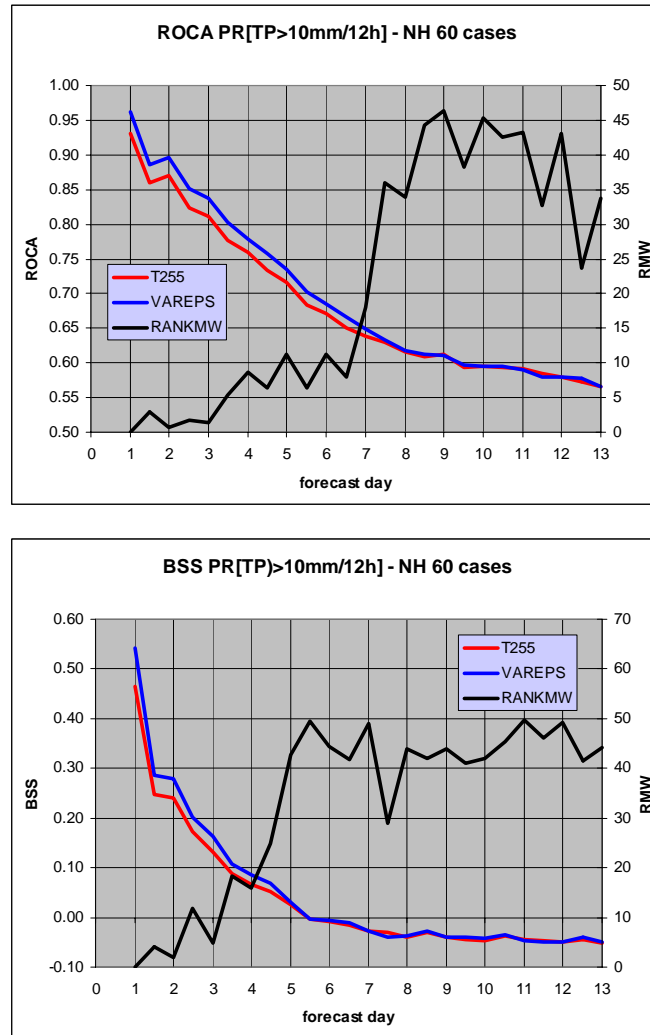


Figure 3. Top panel: 60-case average area under the relative operating characteristic curve (ROCA) for the probabilistic prediction of total precipitation in excess of 10 mm/12h over Northern Hemisphere for EPS (red line, left axis) and VAREPS (blue line, left axis), and value of the rank-sum Mann-Whitney-Wilcoxon significance test (RMW, black line, right axis). Bottom panel: as top panel but for the Brier skill score, computed against climatology.

Figure 4 shows the 60-case average area under the relative operating characteristic curve and the Brier skill score (Wilks 1995) for the probabilistic prediction of positive 850 hPa temperature and 500 hPa geopotential height anomalies, for the T255 and the VAREPS systems, verified against the ECMWF analysis. Results indicate that the difference between these two systems in terms of the prediction of these two other variables still favours the VAREPS, but the RMW test has values below 20% only up to forecast day 5.

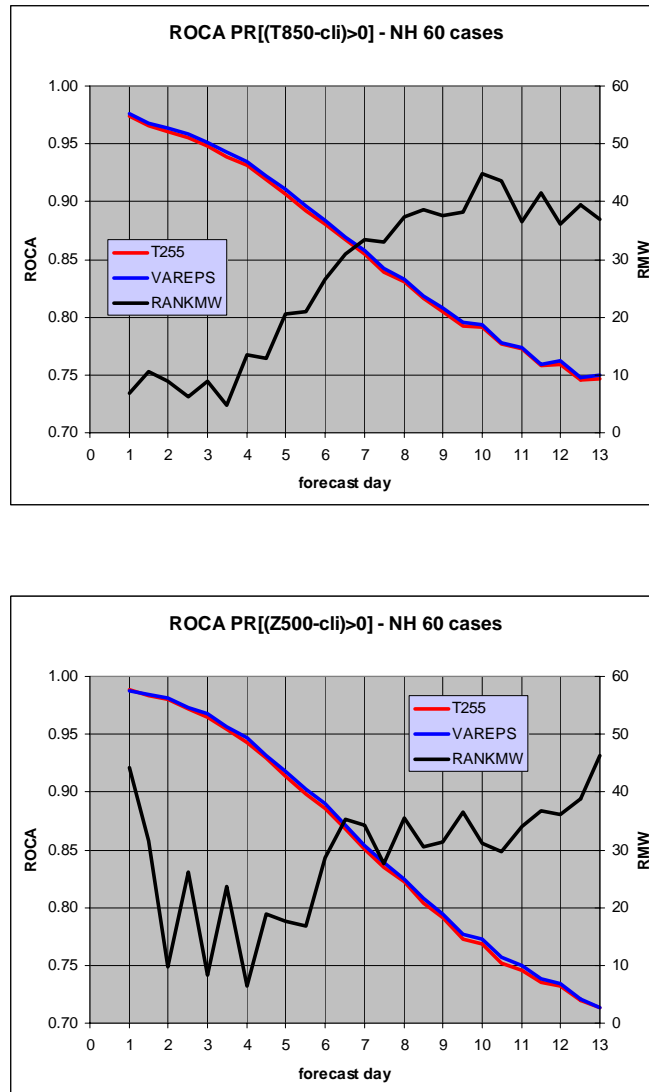


Figure 4. Top panel: 60-case average area under the relative operating characteristic curve (ROCA) for the probabilistic prediction of positive 850 hPa temperature anomalies over Northern Hemisphere for EPS (red line, left axis) and VAREPS (blue line, left axis), and value of the rank-sum Mann-Whitney-Wilcoxon significance test (RMW, black line, right axis). Bottom panel: as top panel but for the ROCA for the probabilistic prediction of positive 500 hPa geopotential height anomalies.

It is worth to point out that the area under the relative operating characteristic for the prediction of both 850 hPa temperature and 500 hPa geopotential height stays above 0.7 for the whole forecast range, suggesting that VAREPS can provide valuable probabilistic forecasts beyond 10 days (note that the current operational EPS stops at forecast day 10).

3.2 Equal-cost comparison: $T_L319(d0-13)$ versus $T_L399(d0-7)+T_L255(d7-13)$

Figure 5 shows the difference between average values (computed for 45 of the 60 cases shown in Figs. 3 and 4) of the area under the relative operating characteristic for three probabilistic forecasts: total precipitation in excess of 10 mm/12h and positive 850 hPa temperature anomalies, for the (equal-cost) VAREPS and T319 configurations. More precisely, each line shows the relative improvement of VAREPS (blue lines) and T319 (yellow lines) with respect to the T255 EPS. Positive/negative relative differences mean that VAREPS/T319 outperforms/underperforms the T255 EPS.

Overall, results indicate first of all that both VAREPS and T319 outperform the T255 EPS, and that although the difference between the VAREPS and the T319 performances is small, VAREPS is associated with a larger relative improvements than T319.

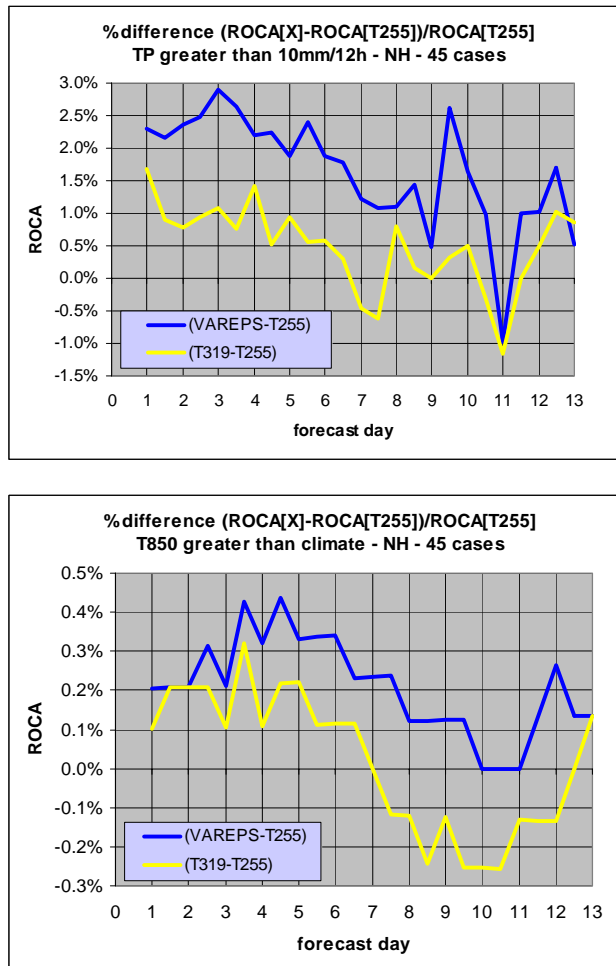


Figure 5. Top panel: differences of 45-case average ROCA for the probabilistic prediction of total precipitation in excess of 10 mm/12h over Northern Hemisphere between VAREPS and T255 (blue line) and between T319 and T255 (yellow line). Bottom panel: as top panel but for the probabilistic prediction of positive 850 hPa positive anomalies.

4 Impact of increased resolution in the short-range for selected cases

The results shown in Figs. 3, 4 and 5 suggest that VAREPS is, on average, a better system than the T_L255 ensemble that was operational up to the end of January 2006 (the average differences are small but statistically significant with a RMW value below 20% up to forecast day 7). Results indicate also that VAREPS is to be preferred to a constant resolution, equal cost T_L319 ensemble. The average results have also indicated that the differences are more detectable in the early forecast range, and especially if one considers fields characterized by small scales features such as total precipitation.

In the next two sections, two synoptic cases are discussed to investigate whether there is any larger positive impact of increasing the resolution in the early forecast range from T_L255 to T_L399 in severe weather events.

4.1 Hurricane Katrina (29 August 2005)

The first case is very recent: hurricane Katrina, one of the strongest storms of the last 100 years. Katrina started to develop as a tropical depression on the 23rd of August south-east of the Bahamas, reached category V on the 28th of August and category IV when it landed on the 29th. At landfall, close to New Orleans, sustained winds of more than 220 km/h were detected.

Figure 6 shows the intensity error (IE) and position error (D) of mean-sea-level-pressure (MSLP) minima predictions by the ensemble members of the T255, the T319 and the VAREPS systems, with an 84, 72, 60 and 48 hour time lead. Ensemble forecasts have been clustered in three categories, accordingly to the intensity and position errors: (IE<5hPa, D<100km), (IE<15hPa, D<200km) and (IE<30hPa, D<300km), with the first category identifying forecasts with very small errors.

Accordingly to this accuracy measure, in 92% of the situations the $T_L399L40$ VAREPS has the highest number of perturbed members with the errors inside the category's limits [more precisely, VAREPS has the highest number for all forecast ranges and for all categories apart for the t+60h forecast for the category (IE<5hPa, D<100km)].

As a consequence of the more accurate development and intensification of the hurricane in each ensemble member, significant wave height (SWH) probabilistic forecasts for the Gulf of Mexico are more accurate in the $T_L399L40$ VAREPS. This can be seen, for example, by comparing the 84-hour probability forecasts of SWH in excess of 8m (Fig. 7): the T255 system gives no probability of SWH exceeding 8m, the T319 system gives a 2-5% probability while the $T_L399L40$ VAREPS system gives a 10-20% probability correctly located in the area where SWH exceeded 8m in the ECMWF operational analysis. Similar differences are detected by comparing probabilistic forecasts for earlier forecast ranges (not shown).

In the case of Katrina, the highest resolution $T_L399L40$ VAREPS system rightly intensified the hurricane development, thus improving probabilistic predictions of other surface variables such as wind speed (not shown) and SWH. But it is worth mentioning that the $T_L399L40$ model does not systematically intensify cyclonic developments. For example, in the case of hurricane Stan, a system that caused severe damage and loss of life in Guatemala because of a land-slide induced by the intense precipitation associated with its passage, the $T_L399L40$ VAREPS forecasts outperformed the $T_L255L40$ and $T_L319L40$ forecasts mostly by positioning more accurately the area affected by the intense precipitation, rather than in the intensification of the cyclone (not shown).

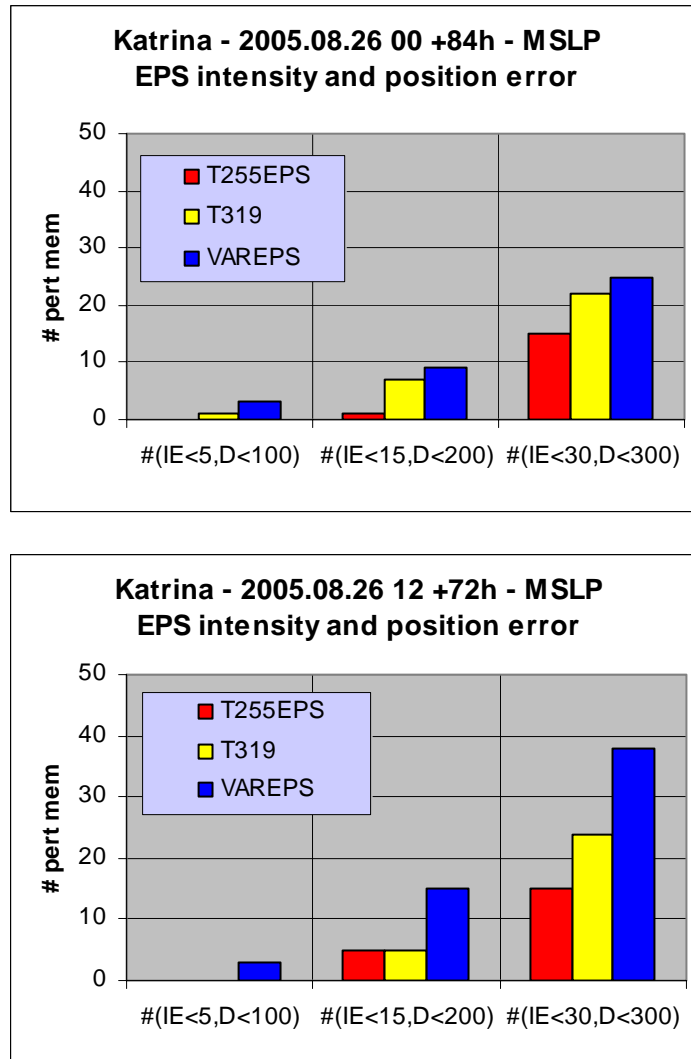


Figure 6. Hurricane Katrina mean-sea-level-pressure (MSLP) intensity and position error statistics for the $T_{L255L40}$ operational EPS, the $T_{L319L40}$ EPS and the $T_{L399L40}$ VAREPS MSLP forecasts valid for 12 UTC of 29 August 2005. $\#(IE<X,D<Y)$ indicates is the number of forecasts with intensity error less than X hPa and position error less than Y km (e.g. $\#(IE<5,D<100)$ indicates is the number of forecasts with intensity error less than 5 hPa and position error less than 100 km. Forecasts have all been verified against the operational $T_{L511L60}$ analysis. Top panel: $t+84h$; bottom panel: $t+72h$.

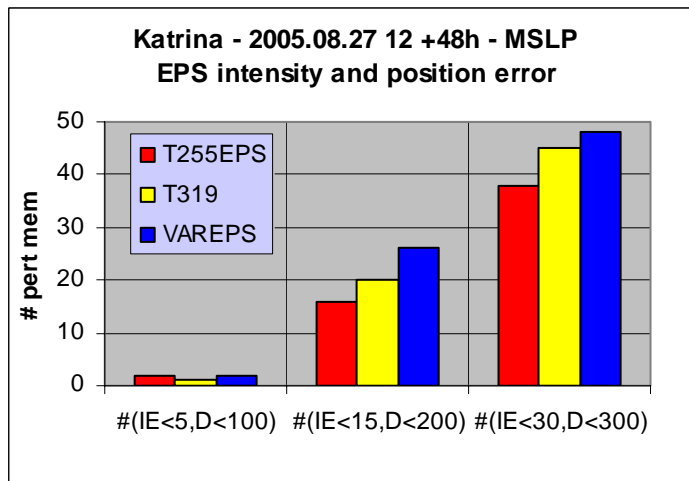
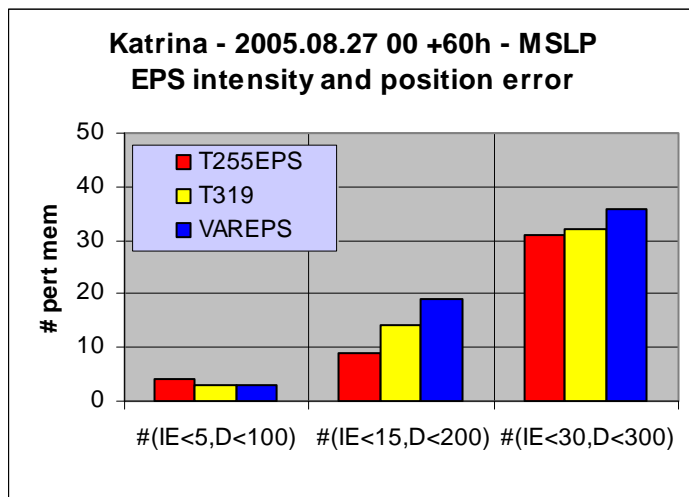


Figure 6 (cont). Top panel: $t+60h$; bottom panel: $t+48h$.

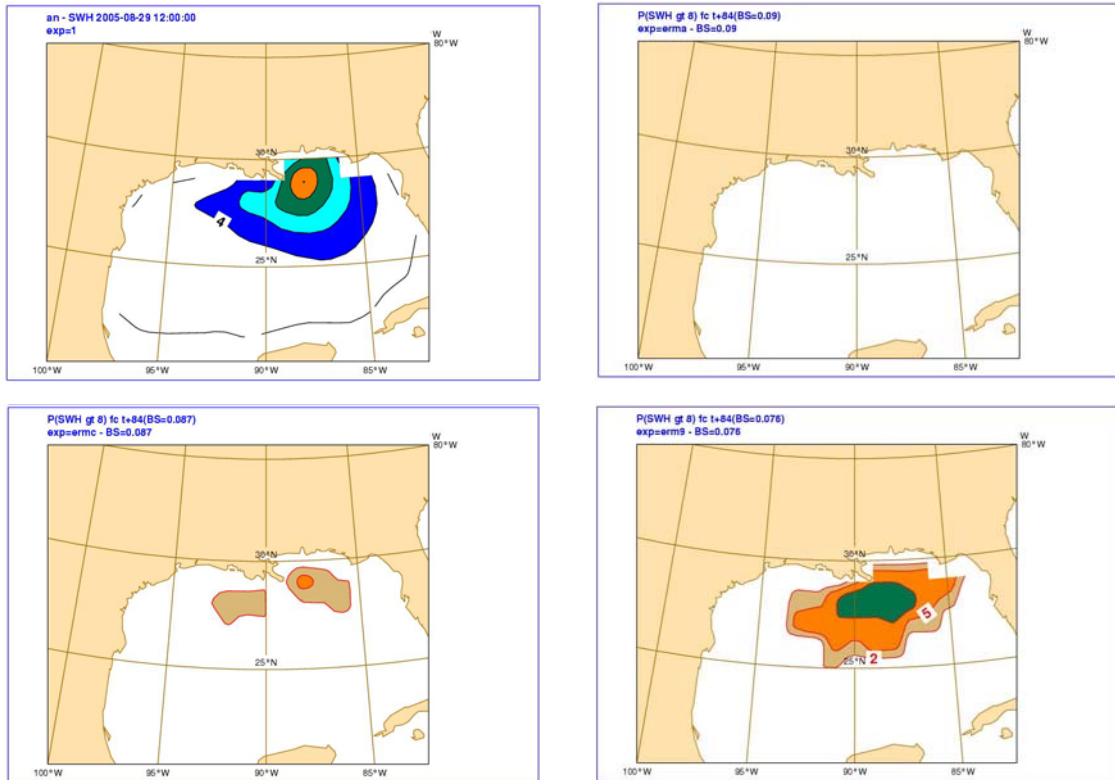


Figure 7. Hurricane Katrina. Top-left panel: significant wave height (SWH) in the operational $T_{L511L60}$ analysis at 12 UTC of 29 August 2005 (contour interval 2m). Other panels: t+84h forecast probability of SWH higher than 8m predicted by the $T_{L255L40}$ operational EPS (top-right), the $T_{L319L40}$ EPS (bottom-left panel) and the $T_{L399L40}$ VAREPS forecast (bottom-right panel). Contour isolines for probabilities are 2, 5 and 10%.

4.2 Firenze flood (4 November 1966, the famous ‘Alluvione di Firenze’)

The second case is a historical one, the flood of North-Eastern and Central Italy of November 1966. This flood event is known as “*l’alluvione di Firenze del ‘66*”, since Firenze was the most famous Italian city affected by it. This flood event, one of the most severe over Europe, caused severe damages to the historical towns of Florence and Venice, disruption in the Po’ Valley and in Tuscany, with loss of lives.

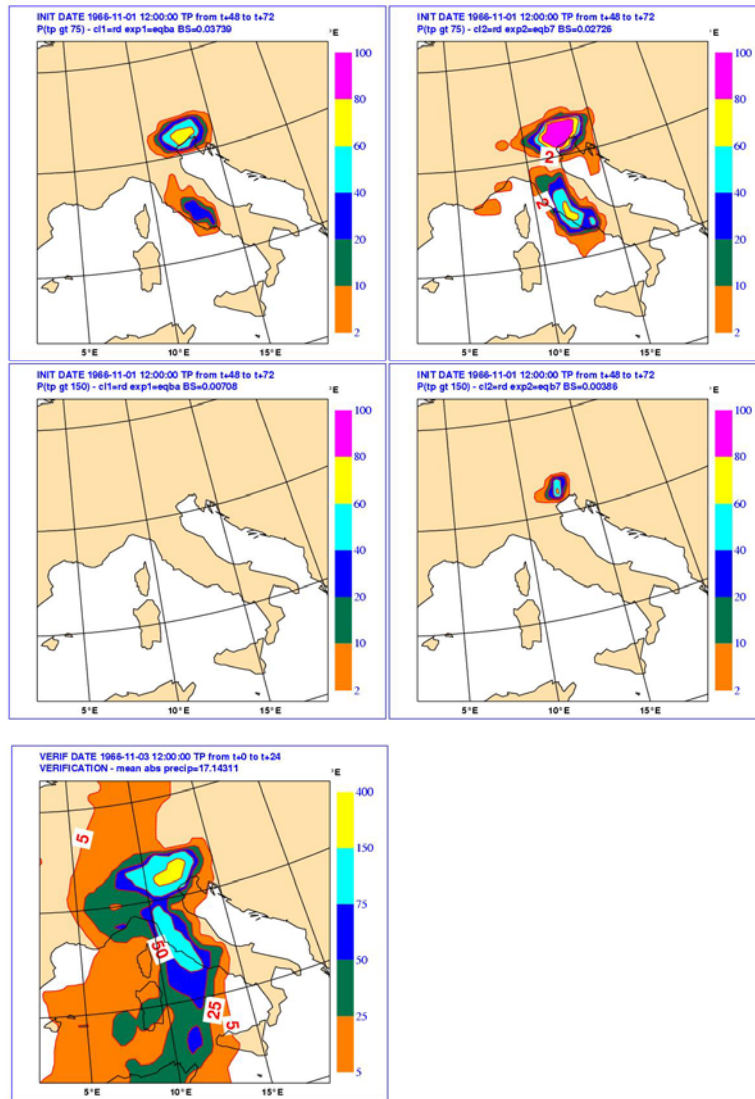


Figure 8.1966 Italian flood +72h probabilistic prediction of 24h accumulated total precipitation (TP) started at 12 UTC of 1 November 1966 and valid for 12 UTC of 4 November, and verification proxy given by the +24h $T_L511L60$ prediction started at 12 UTC of 3 November:

- Top left panel: EPS +72h probabilistic predictions of TP in excess of 75mm/24h
- Top right panel: as top left panel but for the VAREPS prediction
- Middle left panel: EPS +72h probabilistic prediction of TP in excess of 150mm/24h
- Middle right panel: as middle left panel but for VAREPS prediction
- Bottom left panel: verification proxy given by the $T_L511L60$ +24h TP prediction

Contour isolines for probabilities are 2, 10, 20, 4, 60 and 80%, and for TP 5, 25, 50, 75, 150 and 400 mm.

Figure 8 shows the t+48 to t+72 hour probabilistic prediction of total precipitation in excess of 75 and 150mm given by the T_L255 (top and middle left panels) and the T_L399 VAREPS (top and middle right panels) systems valid for the time from 12UTC of the 3rd to the 12UTC of the 4th of November. These probability maps can be compared with the proxy for precipitation verification given by a T_L511L60 forecast started at 12UTC of the 3rd of November (bottom left panel). It is worth mentioning that this proxy field represents rather accurately the overall pattern of the observed precipitation field, but underestimates the maximum values (during the verification period, maximum values of between 200 and 400 mm were observed in Tuscany, and between 300 and 700 mm in North-Eastern Italy, *Malguzzi et al* 2006).

Figure 8 shows that higher probability values are predicted by the T_L399 VAREPS system both over Tuscany and North-Eastern Italy in the areas where intense precipitation was detected. It is interesting to point out that the T_L399 VAREPS gives also a 40-60% probability that precipitation could exceed 150 mm over North-Eastern Italy, correctly pointing out that North-Eastern Italy was going to be affected by most intense rainfall.

5 Planned implementation schedule

The implementation on the 1st of February 2006 of the T_L399L62(d0-10) ensemble prediction system completed the first of a 3-phase upgrading process that will lead to the implementation of the ECMWF Variable Resolution Ensemble Prediction System (VAREPS), designed to increase the ensemble resolution in the early forecast range and to extend the forecast range covered by the ensemble system initially to 15 days and eventually to 32 days, following the planned merging of the ensemble and the monthly operational system.

The second of this 3-phase process, planned for the 2nd half of 2006, will lead to the extension of the 00 and 12 UTC ensemble systems to 15 days using the VAREPS approach, with a T_L399L62 resolution up to forecast day 10 and a T_L255L62 resolution between forecast day 10 and 15.

Results discussed in this report based on the comparison of an earlier version of the VAREPS system with a day-7 (instead of a day-10) truncation have shown the benefits that VAREPS will bring to the users: a system capable to predict more accurately small-scale, severe weather events in the early forecast range and to provide skilful probabilistic predictions of larger scale features in the medium forecast range. Recent results based on the comparison of T_L399L62 and T_L255L62 10-day ensemble, and on VAREPS forecasts with a day-10 truncation (as planned in the operational configuration) have confirmed the results discussed above (not shown).

Finally, details have been provided on the structure of the VAREPS system, including the way forecast data generated by the two VAREPS legs are written in the FDB and are archived in MARS. In particular, it has been pointed out that care must be taken to compute correctly VAREPS forecasts of fields accumulated over a forecast time interval (t_1, t_2) that includes the truncation forecast step t_{TR} (see Appendix A for more information).

6 Acknowledgements

The development, operational implementation, and continuous improvement of the ECMWF Ensemble Prediction System would not have been possible without the contribution of many staff members and consultants: their work is acknowledged.

7 Appendix A - Computation of accumulated fields across the truncation forecast step

Figure 2 shows a schematic of the two legs of each VAREPS forecast. In the Field Data Base (FDB) and in the Meteorological Archival and Retrieval System (MARS), leg-1 data are written in stream=ENFO, while leg-2 data are written in the overlap stream EFOV between forecast day 9 and 10, and in stream ENFO only after day 10. Note that the leg-1 accumulated field at the truncation step t_{TR} interpolated on the T_L255 reduced Gaussian grid, $AF_{var}(t_{TR})$, is also archived in stream EFOV.

Let us introduce the following variables:

- t : forecast step ($0 \leq t \leq 360$)
- $AF(t)$: the accumulated field (accumulated from the start of the forecast) in the FDB/MARS stream ENFO
- $INTERP_{255}[AF(t)]$: the interpolation of $AF(t)$ on the T_L255 reduced Gaussian grid
- $INTERP_{UG}[AF(t)]$: the interpolation of $AF(t)$ on the user's grid
- $AF_{255}(t)$: the $AF(t)$ field interpolated on the T_L255 reduced Gaussian grid:

$$AF_{255}(t) = INTERP_{255}[AF(t)]$$

- $AF_{UG}(t)$: the $AF(t)$ field interpolated on the user's grid (e.g. the T_L255 reduced Gaussian grid, or a regular lat/long grid):

$$AF_{UG}(t) = INTERP_{UG}[AF(t)]$$

- $AF_{var}(t_{TR})$: the leg-1 accumulated field interpolated on the T_L255 Gaussian grid retrieved from stream=EFOV
- $AF_{UG}(t_1, t_2)$: the field accumulated between forecast steps t_1 and t_2 on the user's grid

and let us compute $AF_{UG}(t_1, t_2)$ for all forecast intervals (t_1, t_2) .

If the forecast interval (t_1, t_2) includes the truncation step t_{TR} , $t_1 \leq t_{TR} \leq t_2$ and the user's grid is different from the T_L255 reduced Gaussian grid, the fields archived in the overlap stream should be used to compute correctly $AF_{UG}(t_1, t_2)$, as discussed below in sections A.1, A.2 and A.3. This procedure is necessary because the leg-2 day-10 forecasts (i.e. after 24-hour integration, see Fig. 2) of the accumulated fields are re-set to be equal to the $T_L399L62$ ones interpolated on the T_L255 reduced Gaussian grid.

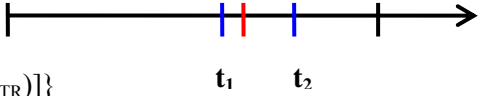
A.1 Computation of accumulated fields on any grid using data in the overlap stream EFOV

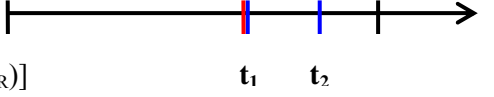
The correct way to compute accumulated fields in the forecast interval (t_1, t_2) is to retrieve fields $AF(t)$ from stream ENFO and $AFvar(t_{TR})$ from stream EFOV on the user's grid, and then compute $AF_{UG}(t_1, t_2)$ as follows:

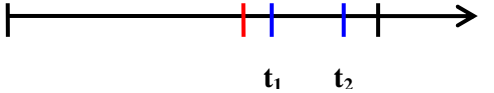
- A) if $t_1 < t_2 \leq t_{TR}$:

$$AF_{UG}(t_1, t_2) = INTERP_{UG}[AF(t_2)] - INTERP_{UG}[AF(t_1)]$$

- B) if $t_1 < t_{TR} < t_2$:

$$AF_{UG}(t_1, t_2) = \{INTERP_{UG}[AF(t_2)] - INTERP_{UG}[AFvar(t_{TR})]\} + \{INTERP_{UG}[AF(t_{TR})] - INTERP_{UG}[AF(t_1)]\}$$

- C) if $t_{TR} = t_1 < t_2$:

$$AF_{UG}(t_1, t_2) = INTERP_{UG}[AF(t_2)] - INTERP_{UG}[AFvar(t_{TR})]$$

- D) if $t_{TR} < t_1 < t_2$:

$$AF_{UG}(t_1, t_2) = INTERP_{UG}[AF(t_2)] - INTERP_{UG}[AF(t_1)]$$


Since in (B) and (C) the fields read in leg-2 to re-set the accumulated fields are explicitly used, this method guarantees that correct accumulated fields are computed.

A.2 Computation of accumulated fields on T_L255 reduced Gaussian grid

Suppose that someone wants the VAREPS accumulated fields $AF(t)$ on the T_L255 reduced Gaussian grid. Then, if the same interpolation is done using the same software that was used to generate $AFvar(t_{TR})$,

$$AF_{UG}(t) = AF_{255}(t) = INTERP_{255}[AF(t)],$$

and for $t = t_{TR}$

$$AF_{UG}(t_{TR}) = AF_{255}(t_{TR}) = INTERP_{255}[AF(t_{TR})] = AFvar(t_{TR}),$$

Thus, the field $AFvar(t_{TR})$ would not be required, and for all (t_1, t_2) :

$$AF_{UG}(t_1, t_2) = AF_{255}(t_2) - AF_{255}(t_1) = INTERP_{255}[AF(t_2)] - INTERP_{255}[AF(t_1)].$$

A.3 Computation of accumulated fields after interpolation to T_L255 reduced Gaussian grid

Suppose that someone wants the VAREPS accumulated fields on a grid that is different from the T_L255 reduced Gaussian grid (e.g. a regular 1-degree latitude-longitude grid), but also wants to avoid

the extraction of the interpolated $AFvar(t_{TR})$ from the overlap stream. This could be achieved by applying a 2-step interpolation procedure:

- First, interpolate all fields on the T_{L255} reduced Gaussian grid [i.e. compute $AF_{255}(t)$] using the same interpolation procedure used to generate the interpolated $AFvar(t_{TR})$. As discussed above, this would guarantee that $AFvar(t_{TR})$ would not be required.
- Then, apply a second interpolation procedure to interpolate the $AF_{255}(t)$ fields from the T_{L255} reduced Gaussian grid to the user's grid

Thus, for all (t_1, t_2) :

$$\begin{aligned} AF_{UG}(t_1, t_2) &= INTERP_{UG}[AF_{255}(t_2)] - INTERP_{UG}[AF_{255}(t_1)] \\ &= INTERP_{UG}[INTERP_{255}[AF(t_2)]] - INTERP_{UG}[INTERP_{255}[AF(t_1)]] \end{aligned}$$

A.4 Use of VAREPS forecasts at a single-point location

It is worth stressing the fact that since the two VAREPS legs are run with different resolution, the corresponding forecast fields are generated using, among others, a different reduced Gaussian grid in physical space, and different land-sea masks and orographies. Users should be aware of this, especially when generating a time-series of VAREPS products for a single location that crosses the truncation forecast step (e.g. when generating a time series of a variable, or an EPS-gramme).

Further reading

- Barkmeijer, J., Buizza, R., & Palmer, T. N., 1999: 3D-Var Hessian singular vectors and their potential use in the ECMWF Ensemble Prediction System. *Q. J. R. Meteorol. Soc.*, **125**, 2333-2351.
- Barkmeijer, J., Buizza, R., Palmer, T. N., Puri, K., & Mahfouf, J.-F., 2001: Tropical singular vectors computed with linearized diabatic physics. *Q. J. R. Meteorol. Soc.*, **127**, 685-708 (also available as ECMWF Technical Memorandum No. 297).
- Buizza, R., & T.N. Palmer, 1995: The singular-vector structure of the atmospheric global circulation. *J. Atmos. Sci.*, **52**, 1434-1456 (also available as ECMWF Technical Memorandum No. 208).
- Buizza, R., T. Petroliaigis, T. N. Palmer, J. Barkmeijer, M. Hamrud, A. Hollingsworth, A. Simmons, & N. Wedi, 1998: Impact of model resolution and ensemble size on the performance of an ensemble prediction system. *Q. J. R. Meteorol. Soc.*, **124**, 1935-1960 (also available as ECMWF Technical Memorandum No. 245).
- Buizza, R., M. Miller, & T. N. Palmer, 1999: Stochastic representation of model uncertainties in the ECMWF ensemble prediction system. *Q. J. R. Meteorol. Soc.*, **125**, 2887-2908 (also available as ECMWF Technical Memorandum No. 279).
- Buizza, R., D. S. Richardson, & T. N. Palmer, 2003: Benefits of increased resolution in the ECMWF ensemble system and comparison with poor-man's ensembles. *Q. J. R. Meteorol. Soc.*, **129**, 1269-1288 (also available as ECMWF Technical Memorandum No. 389).
- Ehrendorfer, M., & Beck, A., 2003: Singular vector-based multivariate sampling in ensemble prediction. ECMWF Technical Memorandum n. 416.
- Janssen P., Bidlot, J.-R., Abdalla, S., & Hersbach, H, 2005: Progress in ocean wave forecasting at ECMWF. ECMWF Technical Memorandum 478.
- Malguzzi, P, Grossi, G, Buzzi, A, Ranzi, R, & Buizza, R, 2006: The 1966 'century' flood in Italy: a meteorological-hydrological revisitation. *J. Geoph. Res.*, under revision.
- Molteni, F., R. Buizza, T. N. Palmer, & T. Petroliaigis, 1996: The ECMWF ensemble prediction system: methodology and validation. *Q. J. R. Meteorol. Soc.*, **122**, 73-119 (also available as ECMWF Technical Memorandum No. 202).
- Saetra, Ø. & Bidlot, J.-R., 2002: Probabilistic forecasts of ocean waves. ECMWF Newsletter, Autumn 2002.
- Untch, A., M. Miller, M. Hortal, R. Buizza, & P. Janssen, 2006: Towards a global meso-scale model: The High Resolution System T_L799L91 & T_L399L62 EPS. ECMWF NewsLetter, June 2006, pg XX-YY.
- Wilks, D. S., 1995: *Statistical methods in the atmospheric sciences*. Academic Press, Inc., San Diego, pp. 467 (ISBN 0-12-751965-3).